Ferrata Storti Foundation

Haematologica 2022
Volume 107(1):154-166

Loss of *Nupr1* promotes engraftment by tuning the quiescence threshold of hematopoietic stem cells via regulation of the p53-checkpoint pathway

Tongjie Wang,[1,2,3,*] Chengxiang Xia,[1,3,*] Qitong Weng,[1] Kaitao Wang,[1] Yong Dong,[1] Sha Hao,[4] Fang Dong,[4] Xiaofei Liu,[1] Lijuan Liu,[1] Yang Geng,[1] Yuxian Guan,[1] Juan Du,[1] Tao Cheng,[4] Hui Cheng[4] and Jinyong Wang[1,2,3]

[1]State Key Laboratory of Experimental Hematology, CAS Key Laboratory of Regenerative Biology, Guangzhou Institutes of Biomedicine and Health, Chinese Academy of Sciences, Guangzhou; [2]Bioland Laboratory (Guangzhou Regenerative Medicine and Health Guangdong Laboratory), Guangzhou; [3]Guangdong Provincial Key Laboratory of Stem Cell and Regenerative Medicine, Guangzhou Institutes of Biomedicine and Health, Chinese Academy of Sciences, Guangzhou and [4]State Key Laboratory of Experimental Hematology & National Clinical Research Center for Blood Diseases, Institute of Hematology & Blood Diseases Hospital, Chinese Academy of Medical Sciences & Peking Union Medical College, Tianjin, China

**TJW and CXX contributed equally as co-first authors.*

ABSTRACT

Hematopoietic stem cells (HSC) are dominantly quiescent under homeostasis, which is a key mechanism of maintaining the HSC pool for life-long hematopoiesis. Dormant HSC are poised to be immediately activated in certain conditions and can return to quiescence after homeostasis has been regained. At present, the molecular networks of regulating the threshold of HSC dormancy, if existing, remain largely unknown. Here, we show that deletion of *Nupr1*, a gene preferentially expressed in HSC, activated quiescent HSC under homeostasis, which conferred a competitive engraftment advantage for these HSC without compromising their stemness or multi-lineage differentiation capacity in serial transplantation settings. Following an expansion protocol, the *Nupr1*$^{-/-}$ HSC proliferated more robustly than their wild-type counterparts *in vitro*. *Nupr1* inhibits the expression of p53 and rescue of this inhibition offsets the engraftment advantage. Our data reveal a new role for *Nupr1* as a regulator of HSC quiescence, which provides insights for accelerating the engraftment efficacy of HSC transplantation by targeting the HSC quiescence-controlling network.

Correspondence:

JINYONG WANG
wang_jinyong@gibh.ac.cn

HUI CHENG
chenghui@ihcams.ac.cn

Received: September 24, 2019.

Accepted: November 25, 2020.

Pre-published: December 10, 2020.

https://doi.org/10.3324/haematol.2019.239186

Introduction

Hematopoietic stem cells (HSC), the seeds of the adult blood system, generate all the blood lineages via hierarchical hematopoiesis. Under steady-state, the majority of HSC are maintained in quiescence, providing a pool of HSC for life-long hematopoiesis.[1] However, the dormant HSC can be rapidly activated for stress hematopoiesis in emergency conditions, such as excessive blood loss, radiation injury, and chemotherapy damage.[2] Mounting evidence points to the existence of an intrinsic molecular machinery of regulating HSC dormancy. In haploinsufficient *Gata2*$^{+/-}$ mice, there is a slight increase of quiescent HSC in conditions of homeostasis.[3] Dnmt3a-knockout HSC have increased self-renewal ability and their number in the bone marrow is increased.[4,5] JunB inactivation deregulates the cell-cycle machinery and reduces quiescent HSC.[6] *Hif-1α*-deficient mice also show a decrease in dormant HSC.[7] Conditional knockout of cylindromatosis (CYLD) induces dormant HSC to exit quiescence and abrogates their repopulating and self-renewal potential.[8] CDK6, a protein not expressed in long-term HSC but present in short-term HSC, regulates exit from quiescence in human HSC, and overexpression of this protein promotes engraftment.[9] Nevertheless, the underlying signaling regulatory network of HSC quiescence remains largely unknown.

Nuclear protein transcription regulator 1 (NUPR1) is a member of the high-mobility group of proteins, which was first discovered in the rat pancreas during the acute phase of pancreatitis and was initially called p8.[10] The same gene was discovered in breast cancer and was named Com1.[11] *NUPR1* has various roles, being involved in apoptosis, stress response, and cancer progression, depending on distinct cellular contexts. In certain cancers, such as breast cancer, *NUPR1* inhibits tumor cell apoptosis and induces tumor establishment and progression.[12-15] In stark contrast, in prostate cancer and pancreatic cancer, *NUPR1* has an inhibitory effect on tumor growth.[16,17] There is accumulating evidence that *NUPR1* is a stress-induced protein: interference of *NUPR1* can upregulate the sensitivity of astrocytes to oxidative stress;[18] loss of it can promote resistance of fibroblasts to adriamycin-induced apoptosis;[19] *NUPR1* mediates cannabinoid-induced apoptosis of tumor cells;[20] and overexpression of *NUPR1* can negatively regulate MSL1-dependent histone acetyltransferase activity in Hela cells, which induces chromatin remodeling and relaxation allowing access of the repair machinery to DNA.[21] Nonetheless, the potential roles of *Nupr1*, which is preferentially expressed in HSC among the hematopoietic stem and progenitor cells, in hematopoiesis remain elusive.

NUPR1 interacts with p53 to regulate cell cycle and apoptosis responding to stress in breast epithelial cells.[19,22] p53 plays several roles in homeostasis, proliferation, stress, apoptosis, and aging of hematopoietic cells.[23-27] Deletion of p53 upregulates HSC self-renewal but impairs the repopulating ability of these cells and leads to tumors.[28] Hyperactive expression of p53 in HSC decreases the size of the HSC pool, and reduces engraftment and deep quiescence.[29-31] These findings support the essential check-point role of p53 in regulating HSC fate. Nonetheless, it is unknown whether NUPR1 and p53 coordinately regulate the quiescence of HSC.

Here, we used a *Nupr1* conditional knockout model to investigate the consequences of loss of function of *Nupr1* in the context of HSC. *Nupr1* deletion in HSC led to the cells exiting from quiescence under homeostasis. In a competitive repopulation setting, *Nupr1*-deleted HSC proliferated robustly and showed dominant engraftment over their wild-type counterparts. *Nupr1*-deleted HSC also expanded abundantly and preserved their stemness *in vitro*. The rescued expression of p53 by *Mdm2*$^{+/-}$ offset the effects introduced by loss of *Nupr1* in HSC. Our studies reveal a new role and signaling mechanism of *Nupr1* in regulating the quiescence of HSC.

Methods

Mice

Animals were housed in the animal facility of the Guangzhou Institutes of Biomedicine and Health (GIBH). *Nupr1*$^{fl/fl}$ mice were provided by Beijing Biocytogen Co., Ltd. CD45.1, Vav-cre, Mx1-cre, and *Mdm2*$^{+/-}$ mice were purchased from the Jackson Laboratory. All the mouse lines were maintained on a pure C57BL/6 genetic background. All experiments were conducted in accordance with experimental protocols approved by the Animal Ethics Committee of GIBH.

Hematopoietic stem cell cycle analysis

We first labeled the HSC with (CD2, CD3, CD4, CD8, Ter119, B220, Gr1, CD48)-Alexa Fluor700, Sca1-Percp-cy5.5, c-kit-APC-cy7, CD150-PE-cy7, CD34-FITC and CD135-PE. The cells were then fixed using 4% paraformaldehyde. After washing, the fixed cells were permeabilized with 0.1% saponin in phosphate-buffered saline together with Ki-67-APC staining for 45 min. Finally, the cells were resuspended in DAPI solution for staining for 1 h. The data were analyzed using Flowjo software.

Bromodeoxyuridine incorporation assay

Nupr1$^{-/-}$ mice and WT littermates were injected with 1 mg bromodeoxyuridine (BrdU) on day 0. They were then allowed to drink water containing BrdU (0.8 mg/mL) *ad libitum*. On days 3, 4, and 5 after the injection of BrdU, four mice of each group were sacrificed. The rate of BrdU incorporation was analyzed by flow cytometry according to the BD Pharmingen™ APC BrdU Flow Kit instructions.

Hematopoietic stem cell culture

The HSC culture protocol has been described elsewhere.[32] Briefly, 50 HSC were sorted into fibronectin (Sigma)-coated 96-well U-bottomed plates directly and were cultured in F12 medium (Life Technologies), 1% insulin-transferrin- selenium-ethanolamine (ITSX; Life Technologies), 10 mM HEPES (Life Technologies), 1% penicillin/streptomycin/glutamine (P/S/G; Life Technologies), 100 ng/mL mouse thrombopoietin, 10 ng/mL mouse stem cell factor and 0.1% polyvinyl alcohol (P8136, Sigma-Aldrich). Half the medium was changed every 2-3 days, by manually removing medium by pipetting and replacing it with fresh medium, as indicated.

Limiting dilution assays

For limiting dilution assays,[33] cells cultured for 10 days were transplanted into lethally irradiated C57BL/6-CD45.1 recipient mice, together with 2×10^5 CD45.1 bone-marrow competitor cells. Recipients were analyzed every 4 weeks. Limiting dilution analysis was performed using ELDA software.[34] based on 1% peripheral blood multilineage chimerism as the threshold for positive engraftment.

Bone marrow competitive repopulation assay

One day before bone marrow transplantation, adult C57BL/6 recipient mice (CD45.1, 8-10 weeks old) were irradiated with two doses of 4.5 Gy (RS 2000, Rad Source) at a 4-hour interval. Bone marrow nucleated cells (BMNC; 2.5×10^5) from *Nupr1*$^{-/-}$ mice (CD45.2) and their WT (CD45.1) counterparts were mixed and injected into irradiated CD45.1 recipients by retro-orbital injection. Control BMNC (CD45.2), *Mdm2*$^{+/-}$*Nupr1*$^{-/-}$ BMNC (CD45.2) or *Mdm2*$^{+/-}$ BMNC (CD45.2) were also mixed with the same number of competitors (CD45.1) and transplanted into recipients. For *Nupr1*$^{fl/fl}$Mx1-cre transplantation, cre expression was induced through intraperitoneal injection of polyinosinic-polycytidylic acid (pI-pC, 250 μg/mouse) every other day 1 week before transplantation. The same number (2.5×10^5) of *Nupr1*$^{fl/fl}$Mx1-cre and WT (CD45.1) BMNC were mixed and transplanted into the lethally irradiated CD45.1 recipients. Mx1-cre$^+$ mice were taken as the experiment control. Mx1-cre and WT (CD45.1) BMNC (2.5×10^5) were used for the transplant control. The transplanted mice were maintained on trimethoprim-sulfamethoxazole-treated water for 2 weeks. For secondary transplantation, BMNC (1×10^6) were obtained from primary competitive transplanted recipients and injected into irradiated CD45.1 recipients (2 doses of 4.5 Gy, 1 day before transplantation). Donor-derived cells and hematopoietic lineages in peripheral blood were assessed monthly by flow cytometry.

Results

Loss of *Nupr1* accelerates the turn-over rates of hematopoietic stem cells under homeostasis

The majority of long-term HSC are quiescent under homeostasis, which is a key mechanism for maintaining the HSC pool for life-long steady hematopoiesis. We hypothesized that genes preferentially expressed in HSC but immediately downregulated in multipotent progenitors (MPP) might form an intrinsic regulatory network for maintaining HSC quiescence. To test our hypothesis, we explored candidate factors by RNA-sequencing analysis of sorted HSC (Lin^- $CD48^-$ $Sca1^+$ $c\text{-}kit^+$ $CD150^+$) and MPP (Lin^- $Sca1^+$ $c\text{-}kit^+$ $CD150^-$). Analysis of differentially expressed genes showed a pattern of transcription factors preferentially present in HSC, including *Rorc*, *Hoxb5*, *Rarb*, *Gfi1b*, *Mllt3*, and *Nupr1*. By literature search, we found that most of the candidate genes except *Nupr1* were reportedly not involved in regulating HSC homeostasis. Thus, we focused on the *Nupr1* gene, the role of which in hematopoiesis has not been reported. The expression of *Nupr1* in HSC was significantly higher (>25-fold, P=0.002) than that in MPP (Figure 1A, left). Real-time polymerase chain reaction (PCR) analysis further confirmed the same expression pattern (P<0.001), indicating an unknown role for *Nupr1* in HSC (Figure 1A, right).

To study whether *Nupr1* has any potential impact on the hematopoiesis of HSC, we created *Nupr1* conditional knockout mice by introducing two loxp elements flanking exons 1 and 2 of the *Nupr1* locus using a C57BL/6 background mESC line (Figure 1B). The resultant $Nupr1^{fl/fl}$ mice were further crossed to Vav-Cre mice to generate $Nupr1^{fl/fl}$; Vav-Cre compound mice ($Nupr1^{-/-}$ mice). The deletion of *Nupr1* was confirmed by PCR in HSC (*Online Supplementary Figure S1A-C*). Adult $Nupr1^{-/-}$ mice (8-10 weeks old) had a normal percentage of blood lineage cells in peripheral blood, including $CD11b^+$ myeloid, $CD19^+$ B, and $CD90.2^+$ T lineage cells (*Online Supplementary Figure S2*). We further investigated the potential alterations of HSC homeostasis in the absence of *Nupr1*. Flow cytometry analysis demonstrated that the $Nupr1^{-/-}$ HSC pool was comparable to the wild-type counterpart in terms of ratios and absolute numbers (*Online Supplementary Figure S3*). Subsequently, we examined the cell cycle status of $Nupr1^{-/-}$ HSC using the proliferation marker Ki-67 and DAPI staining and found that the ratio of $Nupr1^{-/-}$ HSC in G0-status was reduced significantly (P<0.001). Compared with WT HSC (median value: $Nupr1^{-/-}$ HSC =73.67%, WT HSC = 87.15%), more $Nupr1^{-/-}$ HSC entered G1-S-S2 and M phases (Figure 1C, D). To further confirm this novel phenotype, we performed a BrdU incorporation assay, which is conventionally used to assess the turn-over rates of blood cells *in vivo*.[35] The 8-week-old $Nupr1^{-/-}$ mice and littermates were injected intraperitoneally with 1 mg BrdU on day 0, followed by continuous administration of BrdU via water (0.8 mg/mL) for up to 5 days (Figure 1E). After 3 days of BrdU labeling, ~50% of $Nupr1^{-/-}$ HSC became $BrdU^+$ compared with ~35% of WT HSC. The BrdU incorporation rates in HSC differed between the two mouse models (WT and $Nupr1^{-/-}$, P<0.001), and the dynamics changed along with time elapsed (P=0.012, two-way analysis of variance [ANOVA]). Kinetic analysis of BrdU incorporation from day 3 to day 5 revealed that $Nupr1^{-/-}$ HSC contained a 1.5-fold larger $BrdU^+$ population over WT HSC (Figure 1F, G). Collectively, these data indicate that the *Nupr1*-deletion drives HSC to enter the cell cycle and accelerates their turn-over rates in homeostasis.

$Nupr1^{-/-}$ hematopoietic stem cells show repopulating advantage without their multilineage differentiation potential being compromised

To confirm whether $Nupr1^{-/-}$ HSC have a repopulating advantage or disadvantage *in vivo*, we performed a typical HSC competitive repopulation assay. BMNC ($2.5x10^5$) from $Nupr1^{-/-}$ mice (CD45.2) were transplanted into lethally irradiated recipients (CD45.1) along with the same number of WT (CD45.1) competitor cells. Bone marrow cells from littermates ($Vav\text{-}Cre^+$, $CD45.2^+$) were mixed with WT (CD45.1) competitors and transplanted into the recipients as the experiment control (Figure 2A). Sixteen weeks later, $1x10^6$ BMNC from the primary recipients were transplanted into lethally irradiated recipients to assess long-term engraftment. We observed that donor $Nupr1^{-/-}$ cells accounted for ~70% of cells in the primary recipients, while the control cells accounted for 50%-60% in the recipients from the transplantation control assay. $Nupr1^{-/-}$ cells gradually dominated in peripheral blood of recipients over time after transplantation (Figure 2B). In the chimeras, ~70% of myeloid cells and B lymphocytes were $Nupr1^{-/-}$ donor-derived cells, while ~60% of T lymphocytes were from CD45.1 competitive cells (Figure 2C). To further explore whether $Nupr1^{-/-}$ HSC dominated in the HSC pool, we sacrificed the recipients and analyzed HSC 16 weeks after transplantation. The proportion and absolute number of $Nupr1^{-/-}$ HSC were significantly higher (~1.5-fold) than those of the control HSC in primary recipients (Figure 2D, E). Previous research documented that HSC proliferated rapidly at the expense of their long-term repopulating ability.[36-40] Interestingly, consistent with the dominating trend in the primary transplants, $Nupr1^{-/-}$ cells continuously dominated in the peripheral blood of secondary recipients (Figure 3A). $Nupr1^{-/-}$ HSC further occupied up to 90% of the total HSC in the bone marrow of secondary recipients. However, the control HSC accounted for less than 10% in the secondary recipients (Figure 3B, C). Collectively, these results indicate that the deletion of *Nupr1* promotes the repopulating ability of HSC without impairing their long-term engraftment ability.

$Nupr1^{-/-}$ hematopoietic stem cells are highly sensitive to irradiation-stress but re-cover fast

HSC in the cell cycle were reported to be more sensitive to irradiation damage.[41,42] To explore whether $Nupr1^{-/-}$ HSC with a fast turn-over rate are more sensitive to irradiation, WT mice and $Nupr1^{-/-}$ mice were exposed to a single dose of total body irradiation (4 Gy dose, 1 Gy/min). Apoptosis and cell cycle status were analyzed 6 h (early stage) and 24 h (later stage) later. As expected, $Nupr1^{-/-}$ HSC showed a significantly enhanced sensitivity to irradiation: only ~40% of $Nupr1^{-/-}$ HSC lived 6 h after irradiation, whereas ~70% of WT HSC were still alive (*Online Supplementary Figure S4A*). The proportion of radiation-induced apoptosis (annexin V^+) of $Nupr1^{-/-}$ HSC was significantly higher (~2-fold, P=0.02) than that of WT HSC (*Online Supplementary Figure S4A*). Furthermore, ~60% of the residual $Nupr1^{-/-}$ HSC were in G1-S-G2-M proliferative phases compared with ~50% of the residual WT HSC (P=0.01) (*Online Supplementary Figure S4B*), indicating an accelerated replenishment rate in response to irradiation damage. At a later stage (24 h) after irradiation, we observed more living $Nupr1^{-/-}$ HSC (WT *vs.*

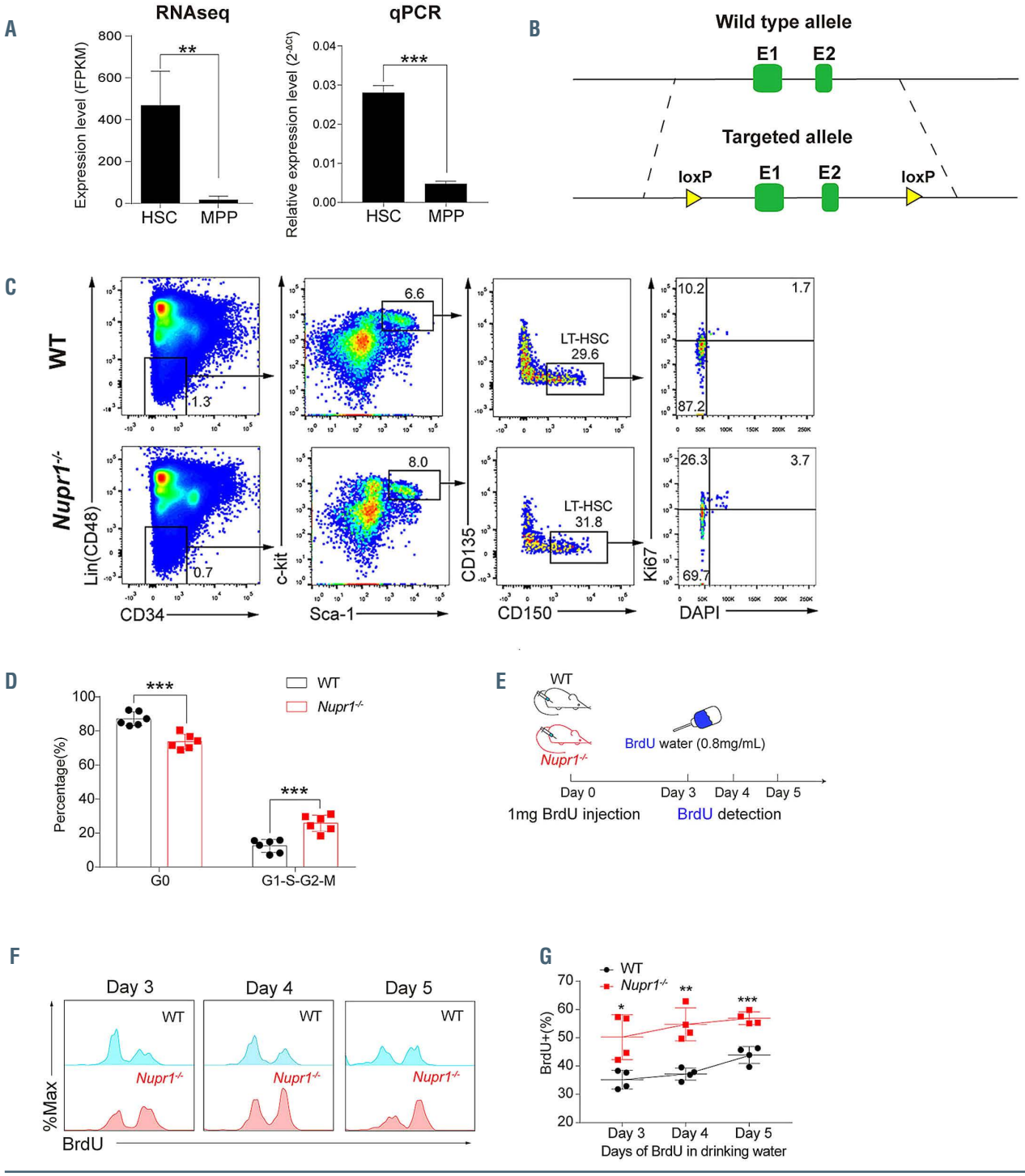

Figure 1. Loss of *Nupr1* activates hematopoietic stem cells that are dormant during homeostasis. (A) Expression pattern of *Nupr1* in hematopoietic stem cells (HSC) and multipotent progenitors (MPP) examined by RNA-sequencing and real-time polymerase chain reaction (qPCR). One thousand HSC or MPP from bone marrow of wild-type (WT) mice were sorted as individual samples for RNA-sequencing (n=4). HSC were defined as Lin^- (i.e., $CD2^-$, $CD3^-$, $CD4^-$, $CD8^-$, $Mac1^-$, $Gr1^-$, $Ter119^-$, $B220^-$), $CD48^-$, $Sca1^+$, $c\text{-}kit^+$, and $CD150^+$. MPP were defined as Lin^-, $Sca1^+$, $c\text{-}kit^+$, and $CD150^-$. Data were analyzed using an unpaired Student t-test (two-tailed) and are represented as mean ± standard deviation (SD) (qPCR, n=3 mice for each group). $^{**}P<0.01$, $^{***}P<0.001$. FPKM: fragments per kilobase of exon per million mapped reads. (B) Targeting strategy for the knockout of the *Nupr1* gene in mice. WT *Nupr1* exons 1 and 2 are shown as green boxes. Two loxp elements flanking exon 1 and exon 2 were inserted. (C) Cell cycle analysis of *Nupr1*$^{-/-}$ HSC under homeostasis. Representative plots of cell cycle from representative WT and *Nupr1*$^{-/-}$ mice (8 weeks old). WT littermates (8 weeks old) were used as controls. HSC (Lin^- $CD48^-$ $Sca1^+$ $c\text{-}kit^+$ $CD150^+$ $CD34^-$ $CD135^-$) were analyzed by DNA content (DAPI) *versus* Ki-67: G0 (Ki-67^{low}DAPI^{2N}), G1 (Ki-67^{high}DAPI^{2N}), G2-S-M (Ki-67^{high}DAPI$^{>2N\text{-}4N}$). (D) Statistical analysis of the HSC cycle. The percentages (%) of HSC in G0 and in G1-G2-S-M stages were analyzed. Data were analyzed using an unpaired Student *t*-test (two-tailed) and are represented as mean ± SD (n=6 mice for each group). $^{**}P<0.01$. (E) The strategy of the BrdU incorporation assay. The 8-week-old *Nupr1*$^{-/-}$ mice and littermates were injected intraperitoneally with 1 mg BrdU on day 0. The mice were then allowed to drink BrdU (0.8 mg/mL) water *ad libitum* until analyzed on days 3, 4, and 5. (F) Dynamic analysis of $BrdU^+$ HSC after BrdU administration, as determined by flow cytometry on days 3, 4, and 5. (G) Kinetics of the $BrdU^+$ HSC ratio. Data were analyzed using an unpaired Student t-test (two-tailed) and two-way analysis of variance and are represented as mean ± SD (n=4 mice for each group). $^{*}P<0.05$, $^{**}P<0.01$, $^{***}P<0.001$.

Nupr1$^{-/-}$: 74% *vs.* 86%) and less irradiation-induced apoptotic *Nupr1*$^{-/-}$ HSC compared with WT HSC (*Online Supplementary Figure S4C*). The proportion of cycling cells (G1-S-G2-M proliferative phases) in the residual *Nupr1*$^{-/-}$ HSC was still significantly higher (P<0.001) than the WT HSC 24 h after irradiation (WT *vs. Nupr1*$^{-/-}$: 29% *vs.* 48%) (*Online Supplementary Figure S4D*). Thus, *Nupr1*$^{-/-}$ HSC were susceptible to irradiation-induced damage, but the surviving HSC proliferated, resulting in a fast recover of the HSC pool.

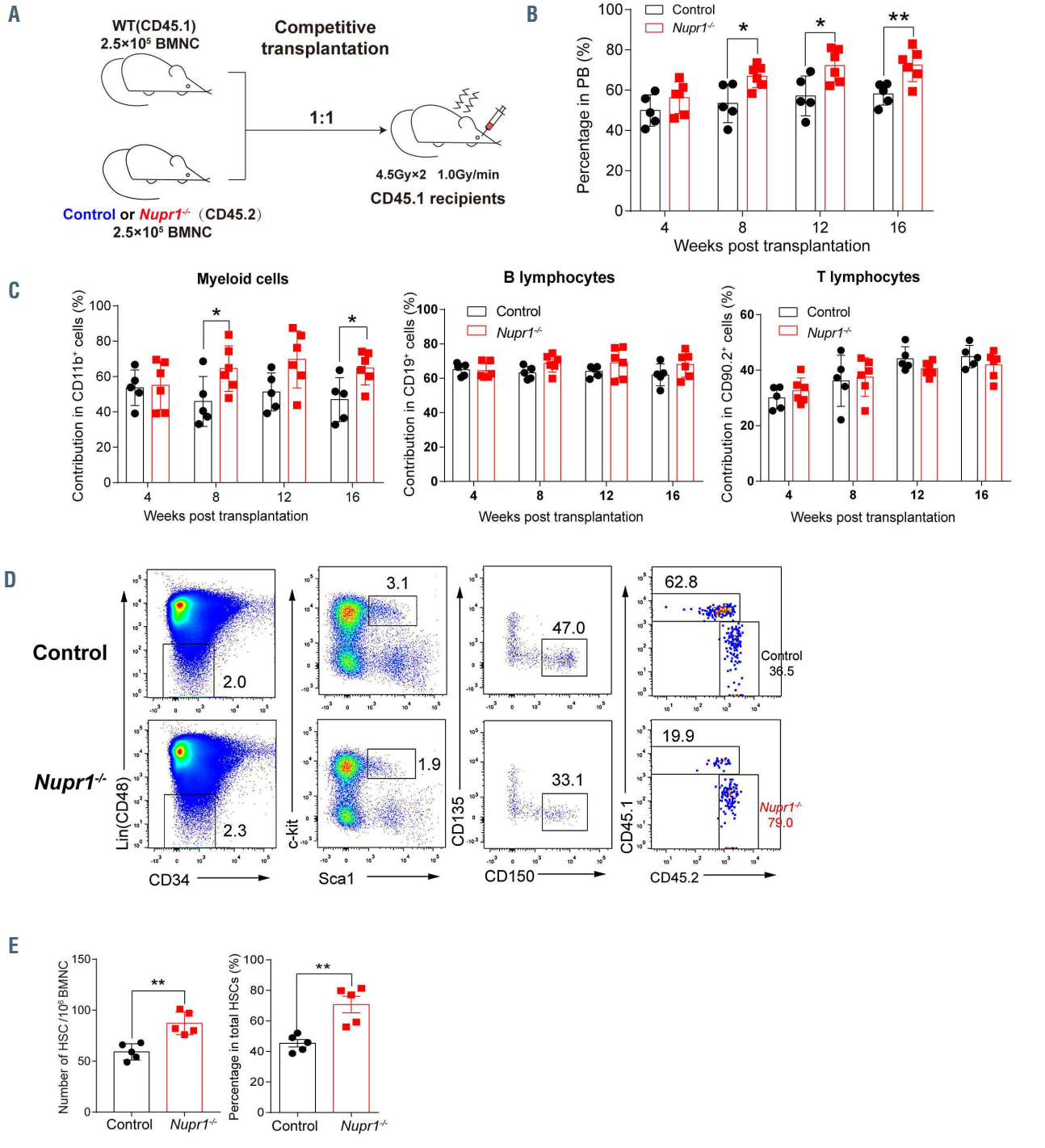

Figure 2. *Nupr1*$^{-/-}$ hematopoietic stem cells show a repopulating advantage in competitive transplantation experiments. (A) Schematic diagram of the competitive transplantation assay. Bone marrow nucleated cells (BMNC; 2.5x10^5) from *Nupr1*$^{-/-}$ (CD45.2) or littermate control (Vav-cre$^+$, CD45.2) mice were mixed with equivalent wild-type (WT) (CD45.1) counterparts and injected into individual lethally irradiated recipients (CD45.1). Four months later, the recipients were sacrificed and 1x10^6 BMNC from primary transplanted recipients were transplanted into lethally irradiated secondary recipients. (B) Kinetic analysis of donor chimerism (CD45.2$^+$) in peripheral blood (PB). Data were analyzed by two-way analysis of variance (ANOVA) and are represented as mean ± standard deviation (SD) (control group: n=5 mice; *Nupr1*$^{-/-}$ group: n=6 mice). *P<0.05, **P<0.01. (C) Kinetic analysis of donor-derived lineage chimerism in PB, including myeloid cells (CD11b$^+$) (left), B lymphocytes (CD19$^+$) (middle), and T lymphocytes (CD90.2$^+$) (right). Data were analyzed using a paired Student *t*-test (two-tailed) and two-way ANOVA and are represented as mean ± SD (control group: n=5 mice, *Nupr1*$^{-/-}$ group: n=6 mice). *P<0.05. (D) Flow cytometry analysis of the hematopoietic stem cell (HSC) compartment in primary recipients 4 months after transplantation. Representative plots from one recipient mouse in each group are shown. (E) Cell number and percentage of donor-derived HSC in primary recipients 4 months after competitive transplantation. Data were analyzed using a Student t-test and are represented as mean ± SD (n=5) **P<0.01.

Nupr1-deleted hematopoietic stem cells expand robustly *in vitro*

We next examined whether the deletion of *Nupr1* could enhance HSC expansion *in vitro*. Fifty HSC sorted from WT and *Nupr1*$^{-/-}$ mice were cultured *in vitro* for 10 days following a recently described protocol[32] (Figure 4A). After 10 days of culture, the WT input cells yielded more than 2.2×10^4 cells, while *Nupr1*$^{-/-}$ HSC produced approximately 5×10^4 total cells ($P<0.001$) (Figure 4B). The colonies derived from *Nupr1*$^{-/-}$ HSC were much larger than those from WT HSC (Figure 4C). Furthermore, we analyzed the phenotypic HSC populations in the expanded cells and found that the absolute number of phenotypic HSC in individual *Nupr1*$^{-/-}$ colonies was 3 times more than WT HSC ($P=0.005$) (Figure 4D, E). To determine whether the quantitative expansion of phenotypic HSC contained net proliferation of functional HSC, we performed competitive repopulating-unit assays,[33] using serial doses of limiting dilutions of the *in vitro*-expanded cells. The WT HSC frequency in the 10-day expanded cells was 1 in 371 cells, which is equivalent to 61 functional HSC, while the *Nupr1*$^{-/-}$ HSC frequency in the 10-day expanded cells was 1 in 190 cells (Figure 4F),[34] which is equivalent to 263 functional HSC ($P=0.045$). Therefore, the deletion of *Nupr1* induced an approximately 4-fold expansion of functional HSC numbers over WT HSC. Thus, deletion of *Nupr1* enhances the expansion ability of HSC *in vitro*.

Reversion of p53 expression offsets the competitiveness of *Nupr1*$^{-/-}$ hematopoietic stem cells

To further investigate the underlying molecular mecha-

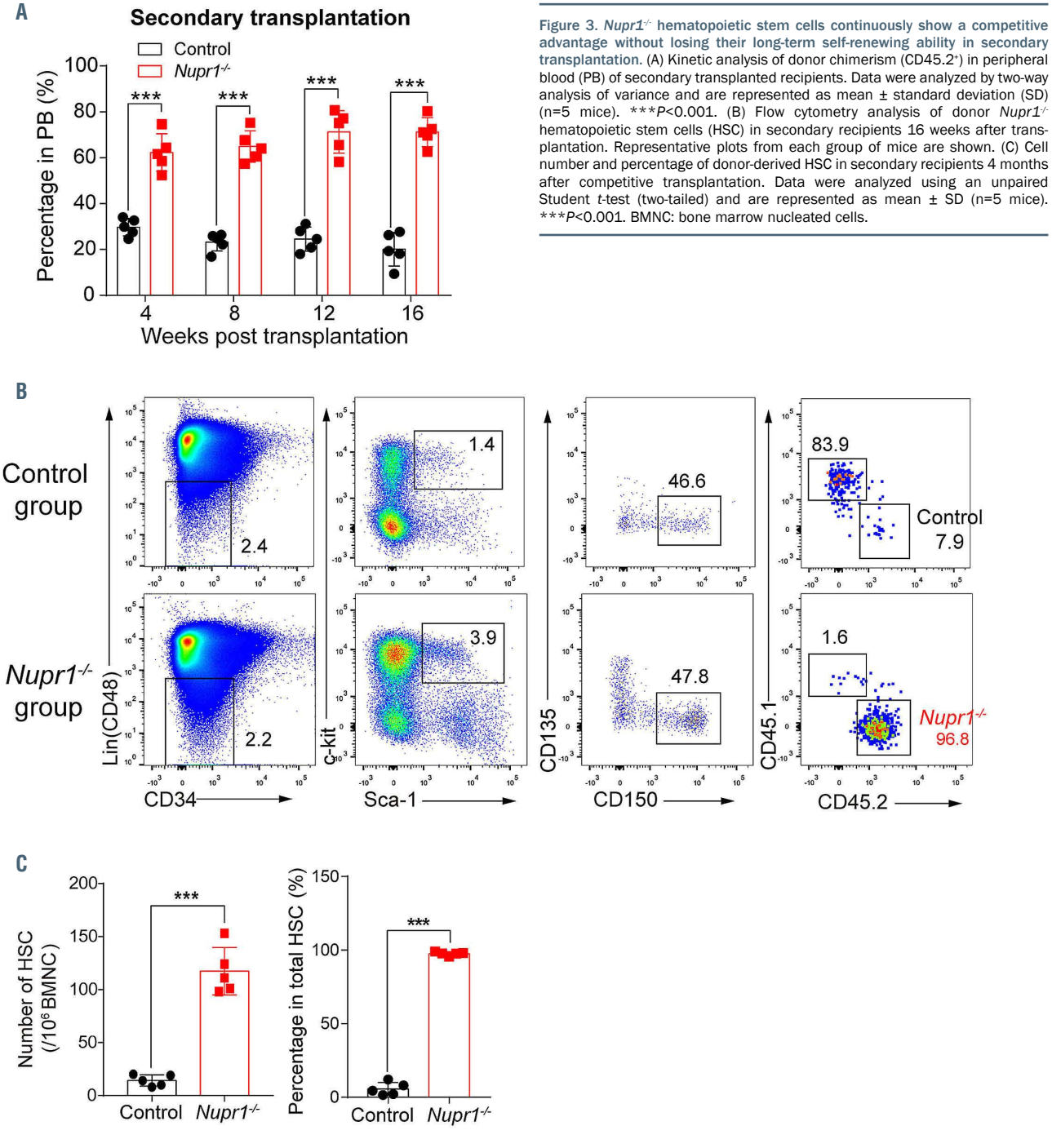

Figure 3. *Nupr1*$^{-/-}$ hematopoietic stem cells continuously show a competitive advantage without losing their long-term self-renewing ability in secondary transplantation. (A) Kinetic analysis of donor chimerism (CD45.2$^+$) in peripheral blood (PB) of secondary transplanted recipients. Data were analyzed by two-way analysis of variance and are represented as mean ± standard deviation (SD) (n=5 mice). ***$P<0.001$. (B) Flow cytometry analysis of donor *Nupr1*$^{-/-}$ hematopoietic stem cells (HSC) in secondary recipients 16 weeks after transplantation. Representative plots from each group of mice are shown. (C) Cell number and percentage of donor-derived HSC in secondary recipients 4 months after competitive transplantation. Data were analyzed using an unpaired Student *t*-test (two-tailed) and are represented as mean ± SD (n=5 mice). ***$P<0.001$. BMNC: bone marrow nucleated cells.

nisms of *Nupr1* in regulating HSC, we performed RNA-sequencing analysis of *Nupr1*$^{-/-}$ HSC from 8-week-old *Nupr1*$^{-/-}$ mice. Analysis of gene expression indicated that there were 319 genes differentially expressed between WT and *Nupr1*$^{-/-}$ HSC (>2-fold difference in expression; adjusted *P* value <0.05 [DESeq2 R package]). Gene-ontology analysis of these differentially expressed genes indicated enrichment of genes involved in regulation of mitotic cell cycle and neg-

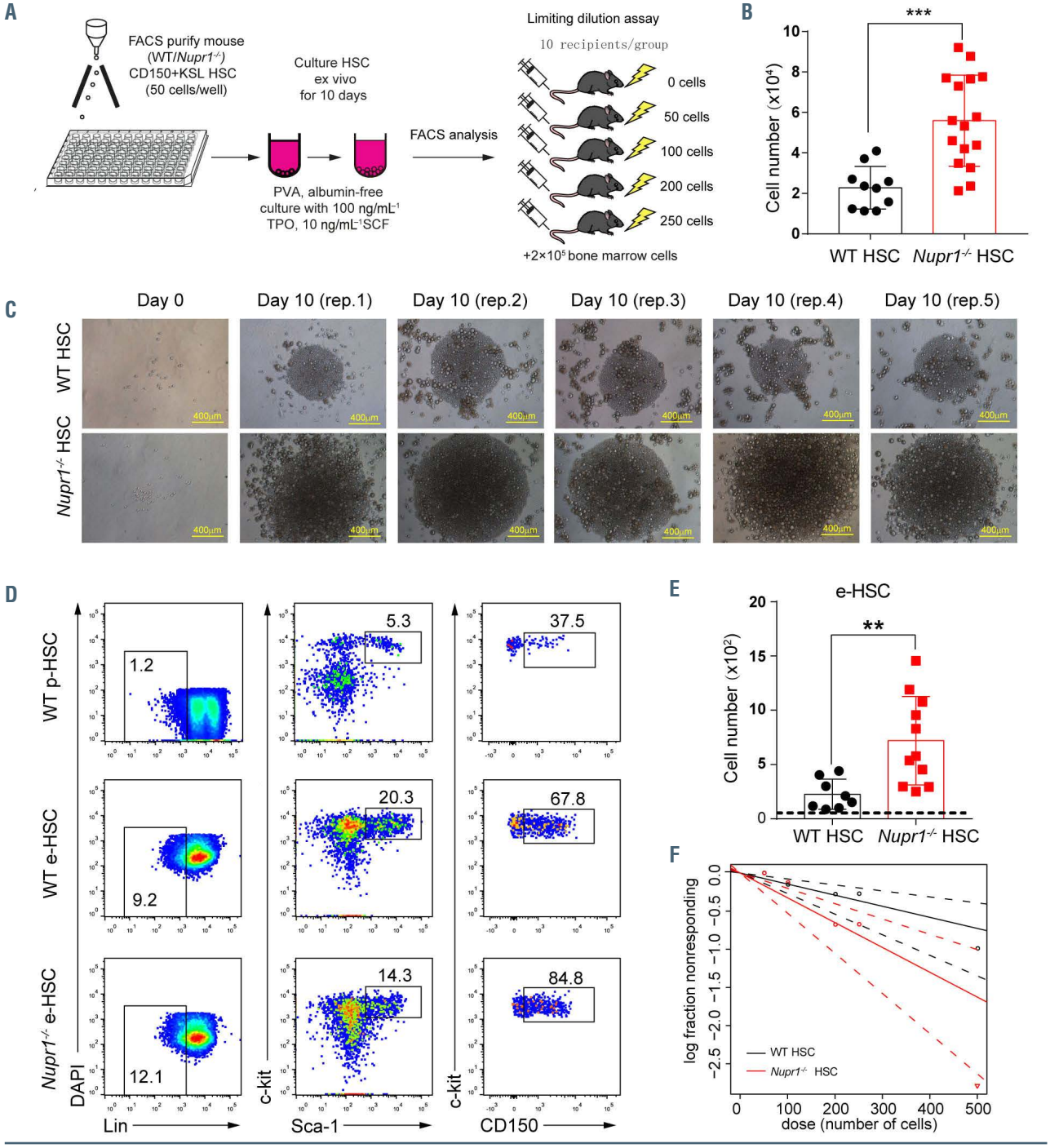

Figure 4. Deletion of *Nupr1* promotes hematopoietic stem cell expansion *in vitro*. (A) Schematic diagram of hematopoietic stem cell (HSC) expansion *in vitro*. Fifty CD150^{+}KSL HSC from wild-type (WT) and *Nupr1*$^{-/-}$ mice were sorted into fibronectin-coated plate wells, containing albumin-free F12 medium supplemented with 1 mg/mL polyvinyl alcohol (PVA), 100 ng/mL thrombopoietin (TPO) and 10 ng/mL stem cell factor (SCF). HSC were cultured for 10 days and then analyzed by flow cytometry (FACS). For the limiting dilution assay, serial doses were transplanted into lethally irradiated recipients, together with 2×10^{5} bone-marrow competitor cells. (B) Number of cells derived from 50 HSC after 10 days of culture *in vitro*. Data were analyzed using an unpaired Student *t*-test (two-tailed) and are represented as mean ± standard deviation (SD) (WT, n=10; *Nupr1*$^{-/-}$, n=16). ***P<0.001. (C) Representative images of WT and *Nupr1*$^{-/-}$ HSC from freshly isolated HSC (day 0) and after 10 days of culture (day 10). Images of five representative colonies (biological replicates) are shown. (D) Representative flow cytometric plots of HSC from cultured WT and *Nupr1*$^{-/-}$ HSC at day 10. p-HSC: primary HSC from bone marrow. e-HSC: expanded HSC after 10 days of culture *ex vivo*. (E) Counts of phenotypic CD150^{+}KSL HSC at day 10 after culture. The dashed line indicates the amount of the primary input cells. Data were analyzed using an unpaired Student *t*-test (two-tailed) and are represented as mean ± SD (WT, n=8; *Nupr1*$^{-/-}$, n=11). **P<0.01. (F) Poisson statistical analysis after limiting-dilution analysis; plots were obtained to allow estimation of competitive repopulating units in each condition (n=10 mice transplanted at each dose per condition, *P<0.05). The plot shows the percentage of recipient mice containing less than 1% CD45.2^{+} cells in the peripheral blood at 16 weeks after transplantation *versus* the number of cells injected per mouse. *P<0.05.

ative regulation of cell cycle (*Online Supplementary Figure S5A, B*). In addition, the positive regulatory genes of cell cycle, such as *Cdk4*, *Cdk6*, *Akt1* and *Akt2*, were upregulated in the *Nupr1*$^{-/-}$ HSC. However, regulators of HSC quiescence, such as *Gfi1*, *Pten*, *Hlf*, *Cdc42* and *Foxo1* were downregulated in the *Nupr1*$^{-/-}$ HSC (*Online Supplementary Figure S5C*).[43,44] Gene set enrichment analysis illustrated that genes related to p53 pathways feedback loops, including *Trp53*, *Ccng1*, *Ctnnb1*, *Pten*, and *Pik3c2b*, were enriched in WT HSC (Figure 5A). The p53 pathway regulates a series of target genes involving cell cycle arrest, apoptosis, senescence, DNA repair, and metabolism.[45] Interestingly, the expression of p53 was significantly reduced (P<0.001) to one-third of the control value in *Nupr1*$^{-/-}$ HSC (Figure 5B). Therefore, we hypothesized that downregulation of p53 in *Nupr1*$^{-/-}$ HSC might account for the competitive advantage of the HSC. MDM2 is a ubiquitin ligase E3 for p53, which is a key repressive regulator of p53 signaling.[46] *Mdm2*-deficient mice showed increased levels of active p53, which is an ideal substitute model of upregulating p53 since directly overexpressing p53 leads to cell death and blood malignancies in mice.[27,47] *Nupr1*$^{-/-}$ mice were crossed with *Mdm2*$^{+/-}$ mice to achieve upregulation of p53 expression in *Nupr1*$^{-/-}$ HSC. As expected, the levels of p53 protein expression in *Nupr1*$^{-/-}$*Mdm2*$^{+/-}$ HSC were comparable to those in WT HSC (P>0.05) but significantly higher than those in *Nupr1*$^{-/-}$ HSC, as measured by indirect immunofluorescence (Figure 5C, D). In addition, most genes involved in the p53 pathway were upregulated in the *Nupr1*$^{-/-}$*Mdm2*$^{+/-}$ HSC, indicated partial recovery of the p53 pathway (*Online Supplementary Figure S6*). We next examined phenotypic HSC in the *Nupr1*$^{-/-}$*Mdm2*$^{+/-}$ mice. Flow cytometry analysis showed that the *Nupr1*$^{-/-}$*Mdm2*$^{+/-}$ HSC pool was indistinguishable from the WT, *Nupr1*$^{-/-}$, and *Mdm2*$^{+/-}$ counterparts in terms of ratios and absolute numbers (Figure 6A, B). Furthermore, we tested the competitiveness of *Nupr1*$^{-/-}$*Mdm2*$^{+/-}$ HSC in parallel with WT, *Nupr1*$^{-/-}$, and *Mdm2*$^{+/-}$ HSC. BMNC (2.5x10^5) from WT, *Nupr1*$^{-/-}$ *Mdm2*$^{+/-}$ mice (CD45.2), *Nupr1*$^{-/-}$ mice (CD45.2), or *Mdm2*$^{+/-}$ mice (CD45.2) were transplanted into lethally irradiated recipients (CD45.1) along with the same number of WT (CD45.1) BMNC. In the recipients of *Nupr1*$^{-/-}$*Mdm2*$^{+/-}$ donor cells, the contribution of *Nupr1*$^{-/-}$*Mdm2*$^{+/-}$ cells was significantly reduced (P<0.001) to ~20%, which was far below the percentage of *Nupr1*$^{-/-}$ cells in recipients of *Nupr1*$^{-/-}$ donor cells, and *Mdm2*$^{+/-}$ cells accounted for less than 10% in the peripheral blood of recipients 16 weeks after transplantation (Figure 6C). Sixteen weeks after transplantation, we also analyzed the *Nupr1*$^{-/-}$*Mdm2*$^{+/-}$ HSC in the

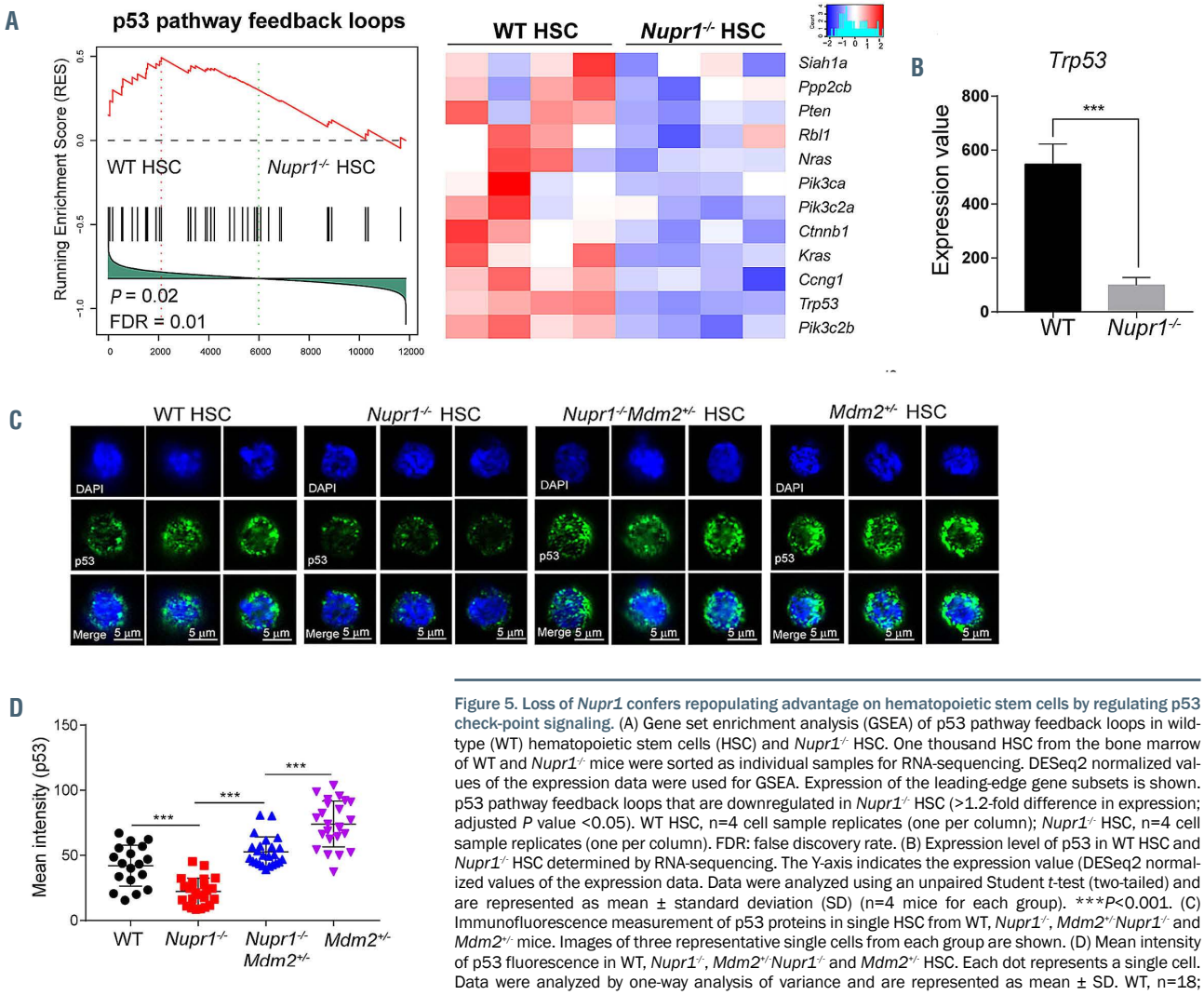

Figure 5. Loss of *Nupr1* confers repopulating advantage on hematopoietic stem cells by regulating p53 check-point signaling. (A) Gene set enrichment analysis (GSEA) of p53 pathway feedback loops in wild-type (WT) hematopoietic stem cells (HSC) and *Nupr1*$^{-/-}$ HSC. One thousand HSC from the bone marrow of WT and *Nupr1*$^{-/-}$ mice were sorted as individual samples for RNA-sequencing. DESeq2 normalized values of the expression data were used for GSEA. Expression of the leading-edge gene subsets is shown. p53 pathway feedback loops that are downregulated in *Nupr1*$^{-/-}$ HSC (>1.2-fold difference in expression; adjusted P value <0.05). WT HSC, n=4 cell sample replicates (one per column); *Nupr1*$^{-/-}$ HSC, n=4 cell sample replicates (one per column). FDR: false discovery rate. (B) Expression level of p53 in WT HSC and *Nupr1*$^{-/-}$ HSC determined by RNA-sequencing. The Y-axis indicates the expression value (DESeq2 normalized values of the expression data. Data were analyzed using an unpaired Student t-test (two-tailed) and are represented as mean ± standard deviation (SD) (n=4 mice for each group). ***P<0.001. (C) Immunofluorescence measurement of p53 proteins in single HSC from WT, *Nupr1*$^{-/-}$, *Mdm2*$^{+/-}$*Nupr1*$^{-/-}$ and *Mdm2*$^{+/-}$ mice. Images of three representative single cells from each group are shown. (D) Mean intensity of p53 fluorescence in WT, *Nupr1*$^{-/-}$, *Mdm2*$^{+/-}$*Nupr1*$^{-/-}$ and *Mdm2*$^{+/-}$ HSC. Each dot represents a single cell. Data were analyzed by one-way analysis of variance and are represented as mean ± SD. WT, n=18; *Nupr1*$^{-/-}$, *Mdm2*$^{+/-}$*Nupr1*$^{-/-}$, *Mdm2*$^{+/-}$: n=25. ***P<0.001.

chimeras. Surprisingly, only a few *Nupr1*$^{-/-}$*Mdm2*$^{+/-}$ HSC were present in the HSC pool of the recipients, while the *Nupr1*$^{-/-}$ HSC dominantly occupied the HSC pool (Figure 6D, E). Overall, the reversal of p53 expression offset the competitive advantage of *Nupr1*$^{-/-}$ HSC.

Deletion of *Nupr1* in adulthood in the *Nupr1*$^{fl/fl}$ Mx1-cre model also promoted hematopoietic stem cell engraftment

In the *Nupr1*$^{fl/fl}$ Vav-Cre model, the *Nupr1* locus was deleted at an embryonic stage. To exclude the possibility that the effects of loss of *Nupr1* observed in adulthood is a consequence of an effect coming from the embryo, *Nupr1*$^{fl/fl}$ mice were crossed with Mx1-Cre mice to generate induced *Nupr1* knockout mice at an adult stage in the presence of polyinosinic-polycytidylic acid (pIpC). The deletion of the *Nupr1* gene in the *Nupr1*$^{fl/fl}$Mx1-cre mice was verified by PCR in HSC (*Online Supplementary Figure S1D, E*). Consistent with the observation of loss of Nupr1 in the *Nupr1*$^{fl/fl}$ Vav-Cre model, significantly more *Nupr1*$^{fl/fl}$Mx1-cre HSC entered the G1-S-S2 and M phases (median value: 26.35%) than their counterparts from littermate control

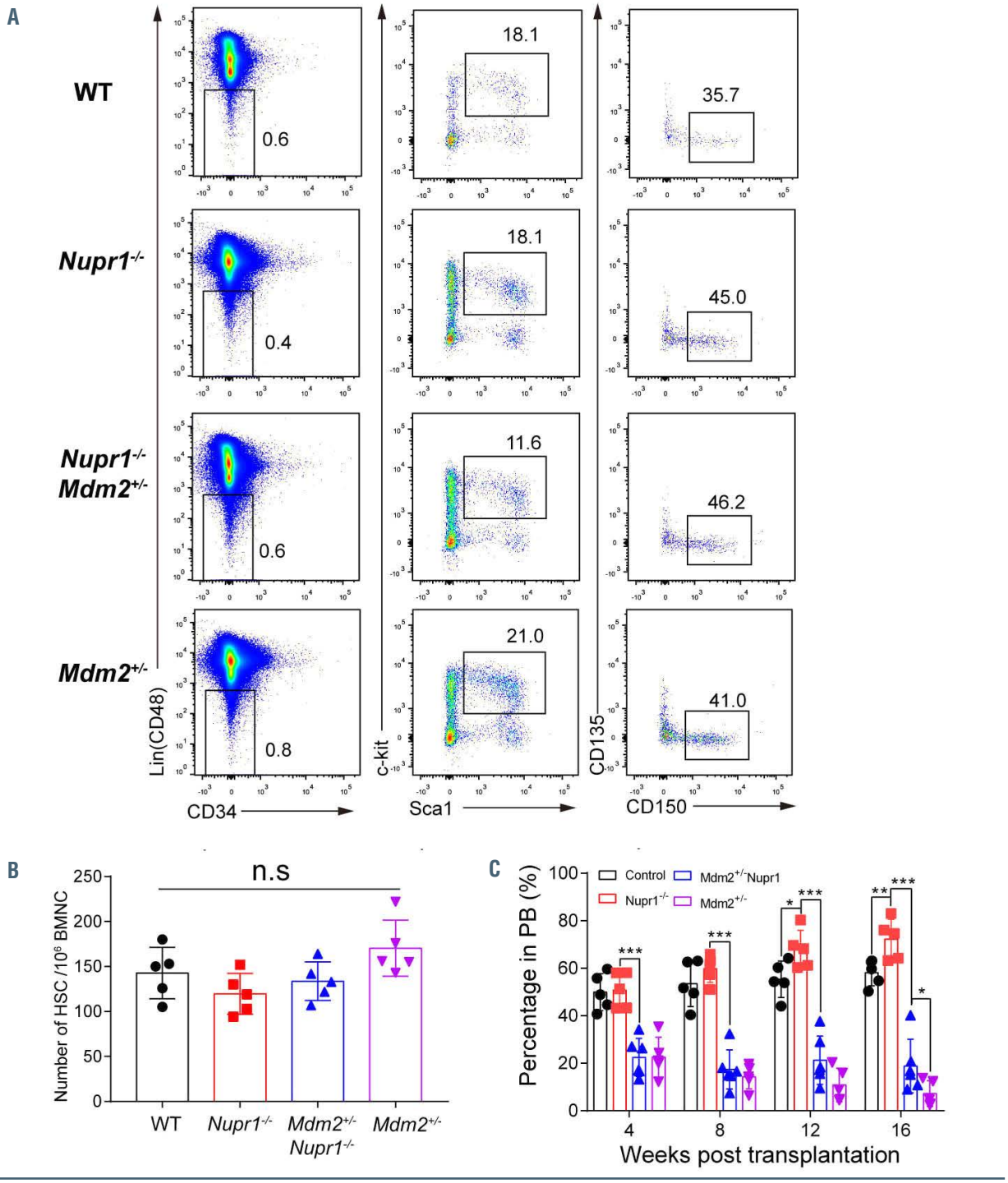

Figure 6. Figure continued on following page.

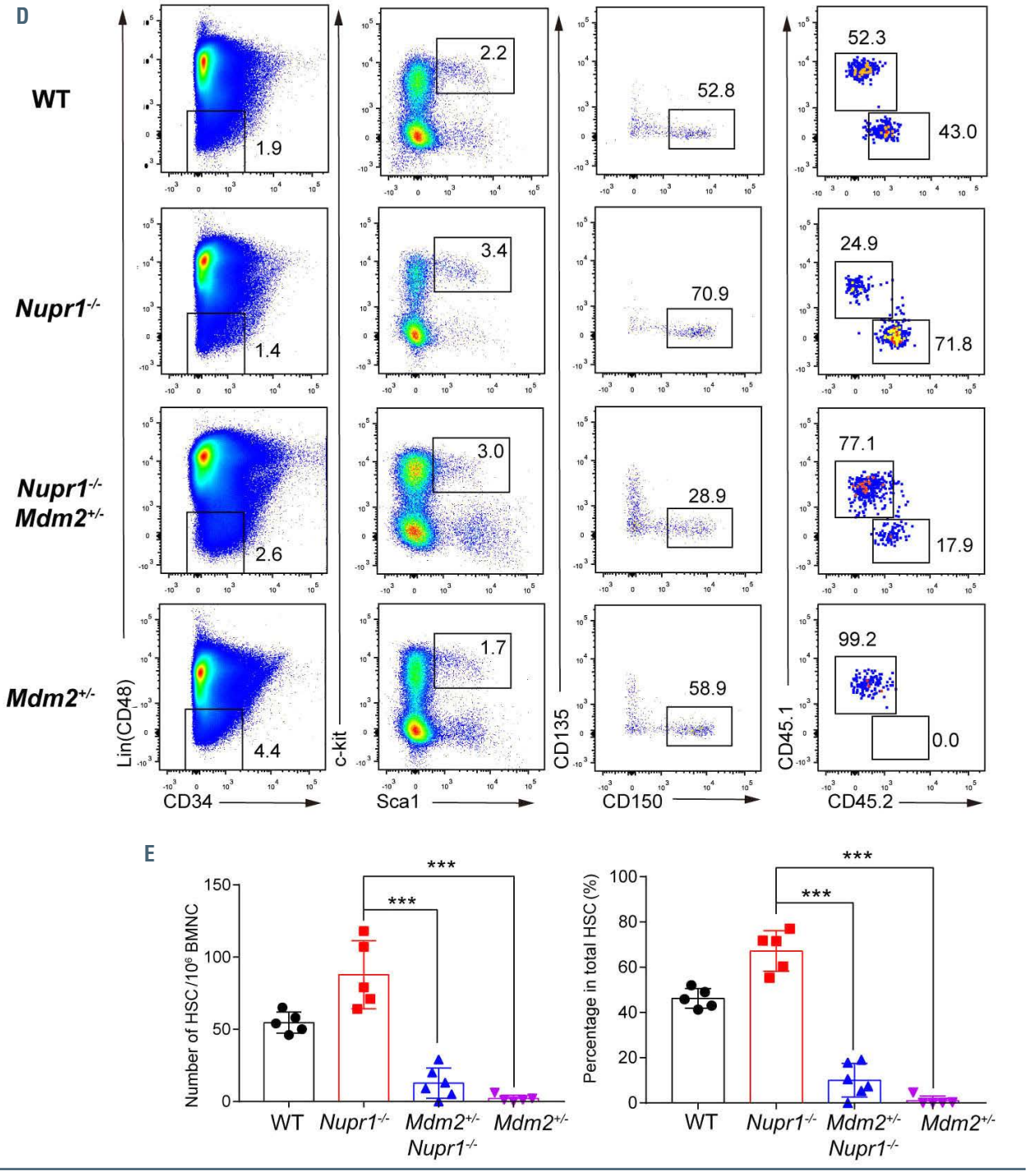

Figure 6. Reversion of p53 expression by allelic depletion of the *Mdm2* gene offsets the repopulating advantage of *Nupr1*$^{-/-}$ hematopoietic stem cells. (A) Representative plots of hematopoietic stem cell (HSC) analysis by flow cytometry from wild-type (WT), *Nupr1*$^{-/-}$, *Nupr1*$^{-/-}$*Mdm2*$^{+/-}$ and *Mdm2*$^{+/-}$ mice bone marrow. (B) Statistical analysis of WT, *Nupr1*$^{-/-}$, *Nupr1*$^{-/-}$*Mdm2*$^{+/-}$ and *Mdm2*$^{+/-}$ HSC number. Data were analyzed by two-way analysis of variance (ANOVA). n=5. BMNC: bone marrow nucleated cells; n.s.: not significant. (C) Donor bone marrow cells (2.5×10^5) from WT (black) *Nupr1*$^{-/-}$ (red), *Nupr1*$^{-/-}$*Mdm2*$^{+/-}$ (blue) (CD45.2) or *Mdm2*$^{+/-}$ (purple) mice were transplanted into lethally irradiated recipient mice (CD45.1) along with 2.5×10^5 recipient bone marrow cells. Data were analyzed using an unpaired Student t-test and are represented as mean ± standard deviation (SD). WT, n=5; *Nupr1*$^{-/-}$, n=5 mice; *Nupr1*$^{-/-}$*Mdm2*$^{+/-}$, n=6 mice; *Mdm2*$^{+/-}$: n=5. **P*<0.05, ****P*<0.001. PB: peripheral blood. (D) Flow cytometry analysis of donor-derived HSC and recipient HSC in bone marrow of recipient mice 4 months after transplantation. HSC were gated as Lin$^-$ (i.e., CD2$^-$, CD3$^-$, CD4$^-$, CD8$^-$, B220$^-$, Gr1$^-$, CD11b$^-$, Ter119$^-$) CD48$^-$ Sca1$^+$ c-Kit$^+$ CD150$^+$ CD34$^-$ CD135$^-$ cells. Plots from one representative mouse of each group are shown. (E) Statistical analysis of the percentage and absolute number of donor-derived HSC in recipient mice 4 months after transplantation. Data were analyzed by one-way ANOVA and are represented as mean ± SD. WT, n=5; *Nupr1*$^{-/-}$, n=5 mice; *Nupr1*$^{-/-}$*Mdm2*$^{+/-}$, n=6 mice; *Mdm2*$^{+/-}$: n=5. ****P*<0.001.

mice (median value: 14.13%, *P*=0.07) (Figure 7A-C). The competitive transplantation result showed that donor *Nupr1*$^{fl/fl}$Mx1-cre cells were advantaged over WT competitors in the peripheral blood of recipients (60%-80%) (Figure 7D). To further investigate whether *Nupr1*$^{fl/fl}$Mx1-cre HSC dominantly occupy recipient bone marrow, we sacrificed the recipients and analyzed the HSC 16 weeks after transplantation. The proportion and absolute number of *Nupr1*$^{fl/fl}$Mx1-cre HSC were significantly greater (~2-fold) than the control HSC competitors in primary recipients

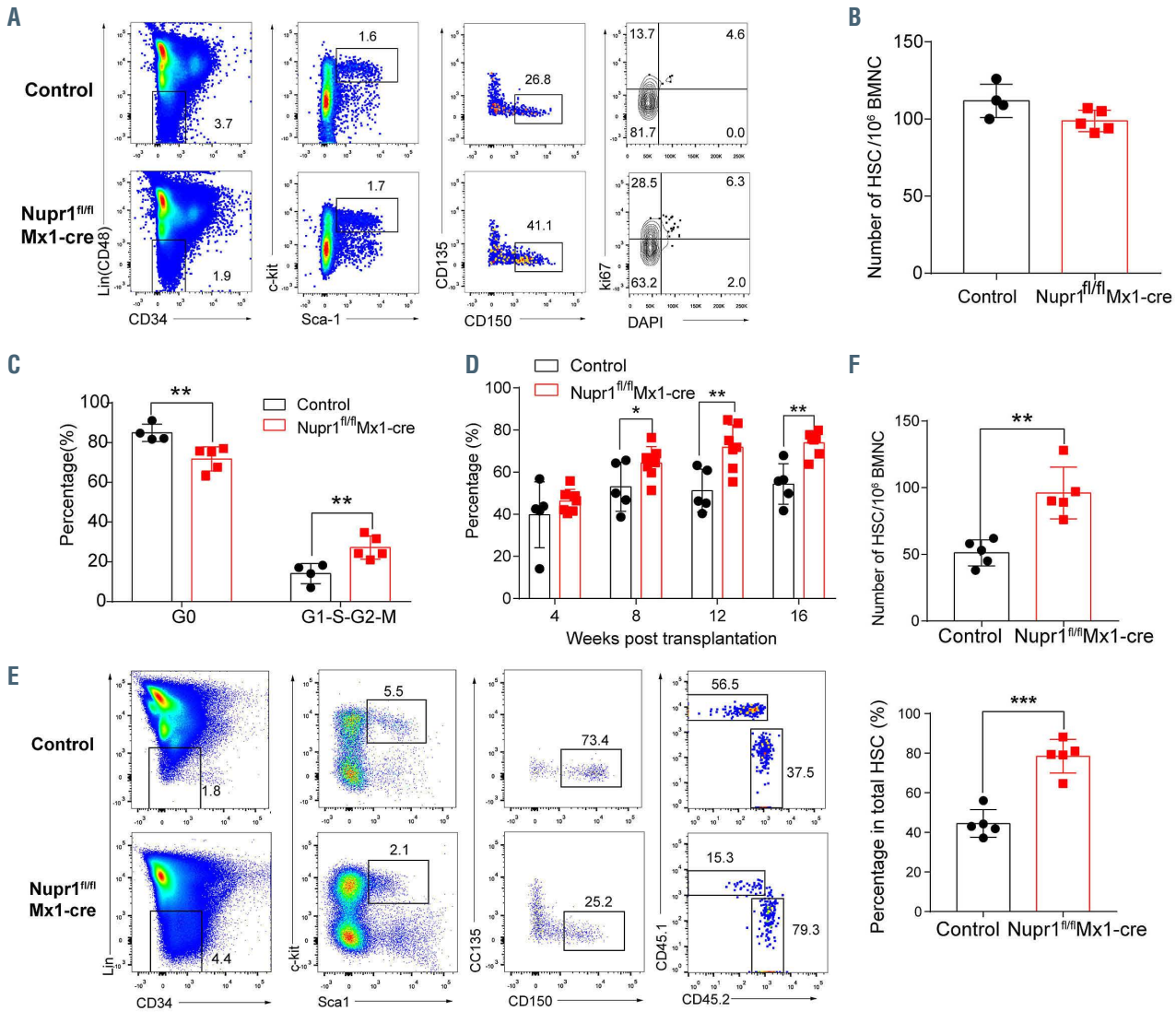

Figure 7. Deletion of *Nupr1* in adulthood promotes hematopoietic stem cell engraftment. (A) Cell cycle analysis of *Nupr1*$^{fl/fl}$Mx1-cre hematopoietic stem cells (HSC) under homeostasis. Representative plots of cell cycle from representative wild-type (WT) and *Nupr1*$^{fl/fl}$Mx1-cre mice (8 weeks old). WT littermates (8 weeks old) were used as controls. HSC (Lin$^-$ (i.e., CD2, CD3$^-$ CD4$^-$ CD8$^-$ B220$^-$ Gr1$^-$ CD11b$^-$ Ter119$^-$) CD48$^-$ Sca1$^+$ c-kit$^+$ CD150$^+$ CD34$^-$ CD135$^-$) were analyzed by DNA content (DAPI) *versus* Ki-67. G0 (Ki-67^{low}DAPI^{2N}), G1 (Ki-67^{high}DAPI^{2N}), G2-S-M (Ki-67^{high}DAPI$^{>2N-4N}$). (B) Statistical analysis of the number of long-term HSC from WT and *Nupr1*$^{fl/fl}$Mx1-cre mice. BMNC: bone marrow nucleated cells. (C) Statistical analysis of the cell cycle of HSC. Ctr: n=4, *Nupr1*$^{fl/fl}$Mx1-cre, n=5. ***P*<0.01. (D) Kinetic analysis of donor chimerism (CD45.2$^+$) in peripheral blood. Data were analyzed by two-way analysis of variance and are represented as mean ± SD (Ctr group: n = 5 mice, *Nupr1*$^{fl/fl}$Mx1-cre group: n =7 mice). ****P*<0.001. (E) Flow cytometry analysis of the HSC compartment in primary recipients 4 months after transplantation. (F) Statistical analysis of donor HSC number and percentage in the transplantation chimeras. Data were analyzed using an unpaired Student *t*-test and are represented as mean ± standard deviation, n=5. ***P*<0.01, ****P*<0.001.

(Figure 7E, F). Thus, in the *Nupr1*$^{fl/fl}$ Mx1-cre model, deletion of Nupr1 in adulthood also promotes HSC engraftment.

Discussion

The intrinsic networks regulating the quiescence of HSC are largely unknown. In this study, loss of *Nupr1* (p8), a gene preferentially expressed in long-term HSC, mildly tuned the quiescence threshold of HSC in the state of homeostasis, without compromising their essential functions in hematopoiesis. *Nupr1* coordinated with p53 to form a signaling machinery regulating HSC quiescence and turnover rates. For the first time, we revealed the new role of *Nupr1* in controlling HSC quiescence.

Nupr1$^{-/-}$ HSC replenished faster than WT HSC under homeostasis. However, the size of the *Nupr1*$^{-/-}$ HSC pool was not altered. These findings imply that despite the existence of intrinsic machinery controlling HSC quiescence, the scale of the HSC pool is also restricted by the extrinsic bone marrow microenvironment.[48] Conventionally, molecules activating HSC produce a transient phenotypic proliferation of HSC but eventually lead to their functional exhaustion and even tumors.[36-40] Interestingly, *Nupr1* signaling seemingly plays a unique role in regulating HSC quiescence and turnover rates, as deletion of *Nupr1* maintained the hematopoietic features of HSC. Consistently, enforced CDK6 expression in HSC confers these cells a competitive advantage without impairing their stemness and multilineage potential.[9] This evidence supports the concept that targeting the intrinsic machinery of balancing the threshold of HSC quiescence might safely promote engraftment.

Loss of *Nupr1* in HSC resulted in an engraftment advantage. In the setting of transplantation stress, the HSC

niche occupied by WT HSC was ablated, providing a niche vacuum into which donor *Nupr1*$^{-/-}$ HSC could enter. The dominance of *Nupr1*$^{-/-}$ HSC is a consequence of faster turnover rates of these cells over their WT counterparts. In a previous study, loss of *Dnmt3a* also led to clonal dominance of HSC, although accompanied by a failure of hematopoiesis due to a dramatic block in differentiation.[4,49] Thus, the engraftment advantage caused by loss of *Nupr1* might have prospective translational implications for HSC transplantation, since a faster recovery of hematopoiesis in HSC transplant hosts definitely reduces infection risks in patients.[50,51]

In our models, *Nupr1* regulated hematopoietic homeostasis via targeting the p53 pathway. p53 is essential for regulating hematopoietic homeostasis.[27] It is unknown whether *NUPR1* interacts directly with p53 in the context of HSC, as commercial antibodies suitable for protein-protein interaction assays are not currently available. *NUPR1* and p53 interacted directly in human breast epithelial cells.[22] Knocking out p53 in HSC can promote HSC expansion, but directly targeting p53 caused HSC apoptosis and tumorigenesis.[52] Thus, *Nupr1* might behave as an upstream regulator of p53 signaling and uniquely regulate cell quiescence in the context of HSC. In a previous study, *Mdm2* was found to be a key repressive regulator of p53 signaling. MDM2 degrades p53 protein by promoting p53 ubiquitination.[46,53] Complete deletion of *Mdm2* will lead to embryonic death because of the excess expression of p53.[46] This embryonic lethality can, however, be rescued by a combination of *Trp53*$^{-/-}$, indicating its essential role of negative regulation of p53. We, therefore, crossed the *Nupr1*$^{-/-}$ mice with *Mdm2*$^{+/-}$ mice in order to upregulate p53 expression indirectly. The level of p53 expression is expectedly elevated in *Nupr1*$^{-/-}$*Mdm2*$^{+/-}$ HSC; however, it is even higher than that in WT mice (Figure 5C, D). A decreased level of MDM2 and increased p53 activity in HSC reduce the ability of competitiveness.[26] Thus, it is possible that the downregulating effect of *Nupr1* on p53 level is mild, while the upregulation of p53 level by haploid deletion of *Mdm2* is dramatic. Consequently, the competitiveness of *Nupr1*$^{-/-}$ *Mdm2*$^{+/-}$ HSC failed to reach WT level in the rescue assay.

In conclusion, loss of *Nupr1* in HSC promotes engraftment by tuning the quiescence threshold of HSC via regulation of the p53 checkpoint pathway. Our study unveils the prospect of shortening the engraftment time-window in HSC transplantation by targeting the intrinsic machinery controlling HSC quiescence.

Disclosures

No conflicts of interest to disclose.

Contributions

TJW and CXX performed research, analyzed data and wrote the paper; YD and QTW analyzed RNA-sequencing data; SH, FD, KTW, XFL, LJL, YG and YXG performed experiments; JD, TC and HC discussed the manuscript; JYW designed the research, and wrote the manuscript.

Funding

This work was supported by grants from the National Natural Science Foundation of China (31900814, 81925002, 81922002), Strategic Priority Research Program of the Chinese Academy of Sciences (XDA16010601), Key Research & Development Program of Guangzhou Regenerative Medicine and Health Guangdong Laboratory (2018GZR110104006), CAS Key Research Program of Frontier Sciences (QYZDB-SSW-SM057), and Science and Technology Planning Project of Guangdong Province (2017B030314056).

References

1. Cheshier SH, Morrison SJ, Liao X, Weissman IL. In vivo proliferation and cell cycle kinetics of long-term self-renewing hematopoietic stem cells. Proc Natl Acad Sci U S A. 1999;96(6):3120-3125.
2. Wilson A, Laurenti E, Oser G, et al. Hematopoietic stem cells reversibly switch from dormancy to self-renewal during homeostasis and repair. Cell. 2008;135(6):1118-1129.
3. Rodrigues NP, Janzen V, Forkert R, et al. Haploinsufficiency of GATA-2 perturbs adult hematopoietic stem-cell homeostasis. Blood. 2005;106(2):477-484.
4. Challen GA, Sun D, Jeong M, et al. Dnmt3a is essential for hematopoietic stem cell differentiation. Nat Genet. 2011;44(1):23-31.
5. Mayle A, Yang L, Rodriguez B, et al. Dnmt3a loss predisposes murine hematopoietic stem cells to malignant transformation. Blood. 2015;125(4):629-638.
6. Santaguida M, Schepers K, King B, et al. JunB protects against myeloid malignancies by limiting hematopoietic stem cell proliferation and differentiation without affecting self-renewal. Cancer Cell. 2009;15(4):341-352.
7. Takubo K, Goda N, Yamada W, et al. Regulation of the HIF-1alpha level is essential for hematopoietic stem cells. Cell Stem Cell. 2010;7(3):391-402.
8. Tesio M, Tang Y, Mudder K, et al. Hematopoietic stem cell quiescence and function are controlled by the CYLD-TRAF2-p38MAPK pathway. J Exp Med. 2015;212(4):525-538.
9. Laurenti E, Frelin C, Xie S, et al. CDK6 levels regulate quiescence exit in human hematopoietic stem cells. Cell Stem Cell. 2015;16(3):302-313.
10. Mallo GV, Fiedler F, Calvo EL, et al. Cloning and expression of the rat p8 cDNA, a new gene activated in pancreas during the acute phase of pancreatitis, pancreatic development, and regeneration, and which promotes cellular growth. J Biol Chem. 1997;272(51):32360-32369.
11. Ree AH, Tvermyr M, Engebraaten O, et al. Expression of a novel factor in human breast cancer cells with metastatic potential. Cancer Res. 1999;59(18):4675-4680.
12. Ree AH, Pacheco MM, Tvermyr M, Fodstad O, Brentani MM. Expression of a novel factor, com1, in early tumor progression of breast cancer. Clin Cancer Res. 2000;6(5):1778-1783.
13. Ito Y, Yoshida H, Motoo Y, et al. Expression and cellular localization of p8 protein in thyroid neoplasms. Cancer Lett. 2003;201(2):237-244.
14. Mohammad HP, Seachrist DD, Quirk CC, Nilson JH. Reexpression of p8 contributes to tumorigenic properties of pituitary cells and appears in a subset of prolactinomas in transgenic mice that hypersecrete luteinizing hormone. Mol Endocrinol. 2004;18(10):2583-2593.
15. Brannon KM, Million Passe CM, White CR, Bade NA, King MW, Quirk CC. Expression of the high mobility group A family member p8 is essential to maintaining tumorigenic potential by promoting cell cycle dysregulation in LbetaT2 cells. Cancer Lett. 2007;254(1):146-155.
16. Jiang WG, Davies G, Martin TA, Kynaston H, Mason MD, Fodstad O. Com-1/p8 acts as a putative tumour suppressor in prostate cancer. Int J Mol Med. 2006;18(5):981-986.
17. Malicet C, Lesavre N, Vasseur S, Iovanna JL. p8 inhibits the growth of human pancreatic cancer cells and its expression is induced through pathways involved in growth inhibition and repressed by factors promoting cell growth. Mol Cancer. 2003;2:37.
18. Malicet C, Giroux V, Vasseur S, Dagorn JC, Neira JL, Iovanna JL. Regulation of apoptosis by the p8/prothymosin alpha complex. Proc Natl Acad Sci U S A. 2006;103(8):2671-2676.
19. Vasseur S, Hoffmeister A, Garcia-Montero A, et al. p8-deficient fibroblasts grow more rapidly and are more resistant to adriamycin-induced apoptosis. Oncogene. 2002;21(11):1685-1694.
20. Carracedo A, Lorente M, Egia A, et al. The stress-regulated protein p8 mediates cannabinoid-induced apoptosis of tumor cells. Cancer Cell. 2006;9(4):301-312.
21. Gironella M, Malicet C, Cano C, et al. p8/nupr1 regulates DNA-repair activity after double-strand gamma irradiation-

induced DNA damage. J Cell Physiol. 2009;221(3):594-602.
22. Clark DW, Mitra A, Fillmore RA, et al. NUPR1 interacts with p53, transcriptionally regulates p21 and rescues breast epithelial cells from doxorubicin-induced genotoxic stress. Curr Cancer Drug Targets. 2008;8(5):421-430.
23. Dumble M, Moore L, Chambers SM, et al. The impact of altered p53 dosage on hematopoietic stem cell dynamics during aging. Blood. 2007;109(4):1736-1742.
24. Lotem J, Sachs L. Hematopoietic cells from mice deficient in wild-type p53 are more resistant to induction of apoptosis by some agents. Blood. 1993;82(4):1092-1096.
25. Shounan Y, Dolnikov A, MacKenzie KL, Miller M, Chan YY, Symonds G. Retroviral transduction of hematopoietic progenitor cells with mutant p53 promotes survival and proliferation, modifies differentiation potential and inhibits apoptosis. Leukemia. 1996;10(10):1619-1628.
26. Bondar T, Medzhitov R. p53-mediated hematopoietic stem and progenitor cell competition. Cell Stem Cell. 2010;6(4):309-322.
27. Liu Y, Elf SE, Miyata Y, et al. p53 regulates hematopoietic stem cell quiescence. Cell Stem Cell. 2009;4(1):37-48.
28. Chen J, Ellison FM, Keyvanfar K, et al. Enrichment of hematopoietic stem cells with SLAM and LSK markers for the detection of hematopoietic stem cell function in normal and Trp53 null mice. Exp Hematol. 2008;36(10):1236-1243.
29. Wang YV, Leblanc M, Fox N, et al. Fine-tuning p53 activity through C-terminal modification significantly contributes to HSC homeostasis and mouse radiosensitivity. Genes Dev. 2011;25(13):1426-1438.
30. Liu D, Ou L, Clemenson GD Jr, et al. Puma is required for p53-induced depletion of adult stem cells. Nat Cell Biol. 2010;12(10):993-998.
31. Yamashita M, Nitta E, Suda T. Regulation of hematopoietic stem cell integrity through p53 and its related factors. Ann N Y Acad Sci. 2016;1370(1):45-54.
32. Wilkinson AC, Ishida R, Kikuchi M, et al. Long-term ex vivo haematopoietic-stem-cell expansion allows nonconditioned transplantation. Nature. 2019;571(7763):117-121.
33. Yamamoto R, Morita Y, Ooehara J, et al. Clonal analysis unveils self-renewing lineage-restricted progenitors generated directly from hematopoietic stem cells. Cell. 2013;154(5):1112-1126.
34. Hu Y, Smyth GK. ELDA: extreme limiting dilution analysis for comparing depleted and enriched populations in stem cell and other assays. J Immunol Methods. 2009;347(1-2):70-78.
35. Kiel MJ, He S, Ashkenazi R, et al. Haematopoietic stem cells do not asymmetrically segregate chromosomes or retain BrdU. Nature. 2007;449(7159):238-242.
36. Motoda L, Osato M, Yamashita N, et al. Runx1 protects hematopoietic stem/progenitor cells from oncogenic insult. Stem Cells. 2007;25(12):2976-2986.
37. Miyamoto K, Araki KY, Naka K, et al. Foxo3a is essential for maintenance of the hematopoietic stem cell pool. Cell Stem Cell. 2007;1(1):101-112.
38. Ficara F, Murphy MJ, Lin M, Cleary ML. Pbx1 regulates self-renewal of long-term hematopoietic stem cells by maintaining their quiescence. Cell Stem Cell. 2008;2(5):484-496.
39. Tipping AJ, Pina C, Castor A, et al. High GATA-2 expression inhibits human hematopoietic stem and progenitor cell function by effects on cell cycle. Blood. 2009;113(12):2661-2672.
40. Campbell TB, Basu S, Hangoc G, Tao W, Broxmeyer HE. Overexpression of Rheb2 enhances mouse hematopoietic progenitor cell growth while impairing stem cell repopulation. Blood. 2009;114(16):3392-3401.
41. Stobbe CC, Park SJ, Chapman JD. The radiation hypersensitivity of cells at mitosis. Int J Radiat Biol. 2002;78(12):1149-1157.
42. Yu H, Shen H, Yuan Y, et al. Deletion of Puma protects hematopoietic stem cells and confers long-term survival in response to high-dose gamma-irradiation. Blood. 2010;115(17):3472-3480.
43. Hao S, Chen C, Cheng T. Cell cycle regulation of hematopoietic stem or progenitor cells. Int J Hematol. 2016;103(5):487-497.
44. Pietras EM, Warr MR, Passegue E. Cell cycle regulation in hematopoietic stem cells. J Cell Biol. 2011;195(5):709-720.
45. Li T, Kon N, Jiang L, et al. Tumor suppression in the absence of p53-mediated cell-cycle arrest, apoptosis, and senescence. Cell. 2012;149(6):1269-1283.
46. Honda R, Tanaka H, Yasuda H. Oncoprotein MDM2 is a ubiquitin ligase E3 for tumor suppressor p53. FEBS Lett. 1997;420(1):25-27.
47. Abbas HA, Maccio DR, Coskun S, et al. Mdm2 is required for survival of hematopoietic stem cells/progenitors via dampening of ROS-induced p53 activity. Cell Stem Cell. 2010;7(5):606-617.
48. Anthony BA, Link DC. Regulation of hematopoietic stem cells by bone marrow stromal cells. Trends Immunol. 2014;35(1):32-37.
49. Challen GA, Sun D, Mayle A, et al. Dnmt3a and Dnmt3b have overlapping and distinct functions in hematopoietic stem cells. Cell Stem Cell. 2014;15(3):350-364.
50. Young JH, Logan BR, Wu J, et al. Infections after transplantation of bone marrow or peripheral blood stem cells from unrelated eonors. Biol Blood Marrow Transplant. 2016;22(2):359-370.
51. Safdar A, Armstrong D. Infections in patients with hematologic neoplasms and hematopoietic stem cell transplantation: neutropenia, humoral, and splenic defects. Clin Infect Dis. 2011;53(8):798-806.
52. Orazi A, Kahsai M, John K, Neiman RS. p53 overexpression in myeloid leukemic disorders is associated with increased apoptosis of hematopoietic marrow cells and ineffective hematopoiesis. Mod Pathol. 1996;9(1):48-52.
53. Haupt Y, Maya R, Kazaz A, Oren M. Mdm2 promotes the rapid degradation of p53. Nature. 1997;387(6630):296-299.